Phys. Med. Biol. 40 (1995) 477–494. Printed in the UK

Large blood vessel cooling in heated tissues: a numerical study

M C Kolios†, M D Sherar‡ and J W Hunt†

† Division of Experimental Therapeutics, The Ontario Cancer Institute and Department of Medical Biophysics, University of Toronto, 500 Sherbourne Street, Toronto, Ontario M4X-1K9, Canada

‡ Division of Clinical Physics, The Ontario Cancer Institute and Department of Medical Biophysics, University of Toronto, 500 Sherbourne Street, Toronto, Ontario M4X-1K9, Canada

Received 30 August 1994, in final form 25 November 1994

Abstract. Large blood vessels can produce steep temperature gradients in heated tissues leading to inadequate tissue temperatures during hyperthermia. This paper utilizes a finite difference scheme to solve the basic equations of heat transfer and fluid flow to model blood vessel cooling. Unlike previous formulations, heat transfer coefficients were not used to calculate heat transfer to large blood vessels. Instead, the conservation form of the finite difference equations implicitly modelled this process. Temperature profiles of heated tissues near thermally significant vessels were calculated. Microvascular heat transfer was modelled either as an effective conductivity or a heat sink. An increase in perfusion in both microvascular models results in a reduction of the cooling effects of large vessels. For equivalent perfusion values, the effective conductivity model predicted more effective heating of the blood and adjacent tissue. Furthermore, it was found that optimal vessel heating strategies depend on the microvascular heat transfer model adopted; localized deposition of heat near vessels could produce higher temperature profiles when microvascular heat transfer was modelled according to the bioheat transfer equation (BHTE) but not the effective thermal conductivity equation (ETCE). Reduction of the blood flow through thermally significant vessels was found to be the most effective way of reducing localized cooling.

1. Introduction

Theoretical, experimental and clinical studies have demonstrated that large blood vessels can produce localized cooling in heated tissues during hyperthermia treatments (Roemer 1991, Lemons *et al* 1987, Levin *et al* 1994). Consequently, an increasing amount of work has been dedicated to the incorporation of large vessel effects in bioheat transfer formulations (Mooibroek and Lagendijk 1991, Chen and Roemer 1992). Most algorithms calculate heat transfer to or from large vessels based on heat transfer coefficients derived from analytical solutions of forced convection in cylindrical ducts (Roemer 1991). Heat transfer coefficients, however, depend on factors that are difficult to incorporate in bioheat transfer algorithms. The coefficients depend on whether the blood is thermally developed (i.e. if the normalized radial temperature profile is independent of axial position (Shah and London 1978)), the perfusion of tissue surrounding the vessel (tissue thermal resistance (Crezee and Lagendijk 1992)), the vessel shape (geometrical factors). Furthermore, heat transfer coefficients vary during transient increases in temperature (Basmadjian 1990) and may vary circumferentially. Therefore, there is a rationale to develop algorithms that do not depend on heat transfer coefficients to calculate heat transfer to and from thermally significant vessels.

0031-9155/95/040477+18$19.50

The number and complex geometry of blood vessels in tissue do not allow one to account for each vessel individually, and thus continuum models are used to model heat transfer in the microcirculation. Continuum models average the effects of many blood vessels in order to predict a local average temperature (Baish 1992). Two continuum models traditionally used are the Pennes bioheat transfer equation (BHTE) and the effective thermal conductivity equation (ETCE). The applicability of these microvascular bioheat transfer formulations is controversial. Recent experimental studies however support both the ETCE (Crezee and Lagendijk 1990) and the BHTE models (Moros *et al* 1993a). It is not clear which model is a better approximation and under what conditions, therefore both models are examined here.

In this work, the conjugate heat transfer problem (i.e. modelling temperatures in tissue and blood regions) is solved numerically without using heat transfer coefficients, in a manner similar to the one proposed by (Moros *et al* 1993b). The blood and tissue domains are modelled by two equations, which for cylindrical coordinates and axial flow become

$$\rho_b c_b \frac{\partial T}{\partial t} + \rho_b c_b u(r) \frac{\partial T}{\partial z} = k_b \left(\frac{\partial^2 T}{\partial^2 r} + \frac{1}{r} \frac{\partial T}{\mathrm{d}r} + \frac{\partial^2 T}{\partial^2 z} \right) + P_b \tag{1}$$

$$\rho_t c_t \frac{\partial T}{\partial t} = k_{\mathrm{eff}} \left(\frac{\partial^2 T}{\partial^2 r} + \frac{1}{r} \frac{\partial T}{\mathrm{d}r} + \frac{\partial^2 T}{\partial^2 z} \right) - w_b c_b (T(r,z) - T_{\mathrm{art}}) + P_t \tag{2}$$

where ρ is the density (g cm^{-3}), c is the specific heat capacity (J g^{-1} per °C), T is the temperature (°C), $u(r)$ is the velocity of blood (cm s^{-1}), k is the thermal conductivity (W cm^{-1} per °C), P is the volumetric power deposition rate (W cm^{-3}), w is the volumetric perfusion rate (g cm^{-3} s^{-1}) and k_{eff} is the tissue effective conductivity for the ETCE. Subscripts art, b and t denote arterial, blood and tissue, respectively. Equation (1) models the convective effects of thermally significant vessels while equation (2) the effects of tissue and microvascular heat transfer.

Temperature profiles of heated tissues close to a thermally significant vessel are calculated with microvascular cooling modelled by the BHTE or ETCE models. Furthermore, to directly compare the simulation results, the values of w_b for the BHTE and k_{eff} for the ETCE model are assigned equivalent values according to experimentally derived data in fixed bovine kidneys (Crezee and Lagendijk 1990). Radial and axial temperature profiles are examined. Finally, strategies to minimize large vessel cooling for steady-state hyperthermia are examined: increasing the power deposition near the vessel, using a modality that heats blood as effectively as tissue and partial occlusion of the blood vessel.

2. Numerical methods

Equations (1) and (2) were solved by the method of finite differences. The conductive terms were discretized according to central differences, while the convective terms according to upwind differences (Patankar 1980). The resulting system of equations was solved using the alternate direction implicit (ADI) method allowing steady state and transient modelling (Ames 1977). The conductivity discontinuities at the vessel–tissue interface for the ETCE model were dealt with by using the harmonic mean of the vessel and tissue conductivities (Patankar 1980). Grid points were concentrated near the vessel region by linearly increasing the radial step size from the vessel centre. The number of radial nodes used was typically 600 and the number of axial nodes 300. The axial step size was 1 mm while the radial step size varied from 3.6×10^{-4} mm to 0.2 mm. The simulations were completed in 2 to 9 h, depending on the problem settings. The numerical methods are compared against benchmark problems in appendix A demonstrating good accuracy. Simulations were performed on either a Silicon

Graphics (4D/440 VGX and Onyx series) or an IBM RISC-6000 computer. Further details on the numerical methods can be found elsewhere (Kolios *et al* 1994).

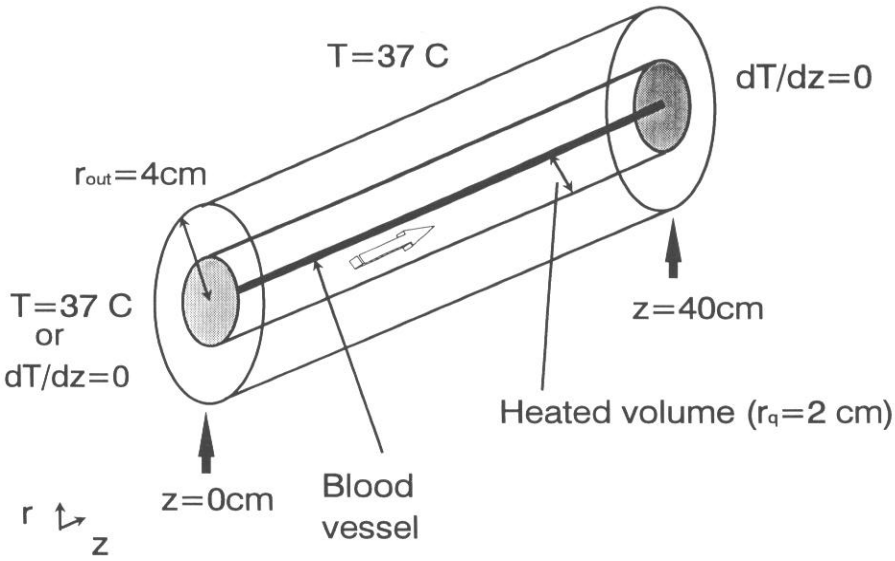

Figure 1. Computer simulation geometry. Three concentric cylinders represent the tissue volume (r_{out} = 4 cm), heated region (r_q = 2 cm) and the blood vessel (r = variable). Uniform power deposition is assumed throughout the entire heated field, apart from the blood vessel.

The geometry used for the simulations is shown in figure 1 and consists of three distinct concentric cylinders, the innermost representing a large blood vessel, the intermediate the actively heated volume and the outer the untreated tissue. The thermally significant vessel is located at the centre of the cylinder, within a heated volume of radius 2 cm representing a hypothetical case of tissue heating. The heated volume is enclosed in unheated tissue and the outer radial boundaries are kept at body temperature. The entrance to the field was set either to body temperature or to an adiabatic condition ($\partial T/\partial z = 0$). An adiabatic condition was implemented for the exit. Uniform power absorption was assumed throughout the entire heated field representing an idealized flat beam. The absorption in the blood vessel region was set to zero, consistent with ultrasound heating. The vessel diameter (δ) and average velocity ($\langle u \rangle$) were assigned physiological values (table 1) and represent vessels considered thermally significant according to previous analytical studies (Crezee and Lagendijk 1992). A parabolic blood velocity profile was assumed which is a reasonable approximation for the vessel sizes considered in this study. A list of the input physical parameters is given in table 2. For the BHTE, perfusion values ranged from 0 to 0.07 g cm^{-3} s^{-1}, spanning the range of volumetric perfusion rates encountered in the human body. The effective conductivity was assigned values ranging from 0.006 (unperfused muscle tissue) to 0.18 W cm^{-1} per °C. To facilitate the comparison of profiles, all data were normalized to the maximum temperature in the heated field. The normalized temperature profiles were independent of the specific absorption rate magnitude (SAR) for both models, allowing the comparison (since the equations are linear).

The expression used to correlate effective conductivity and volumetric perfusion was

$$k_{\text{eff}} = k_t (1 + \alpha' w_b) \tag{3}$$

Table 1. Significant vessel diameters and average flow rates (Crezee and Lagendijk 1992, Chato 1980). Vessel flow values linearly extrapolated for vessel diameters not found in references.

Blood vessel diameter (mm)	Average velocity (cm s^{-1})
2	20
1.4	10.5
1	8
0.8	7.5
0.6	6.0
0.4	5.5
0.2	3.4

Table 2. Listing of physical parameters used in simulations (Duck 1990).

Tissue specific heat capacity (J g^{-1} per °C)	4.180
Tissue density (g cm^{-3})	1.000
Tissue conductivity (W cm^{-1} per °C)	0.006
Blood specific heat capacity (J g^{-1} per °C)	4.180
Blood density (g cm^{-3})	1.000
Perfusion rate (g cm^{-3} s^{-1})	variable

where α' is an empirical parameter (0.12 ml min^{-1} per 100 g) (Crezee and Lagendijk 1992). Linear relations between effective conductivity and volumetric perfusion have also been found by others (Dutton 1993, Bowman *et al* 1989).

3. Results

A typical tissue temperature profile is shown in figure 2. The increase in tissue temperature is a result of the power deposition; cooling in the centre of the cylinder is due to the effects of the blood vessel. At the edges of the field the temperature decays to the body-core temperature. Thermal equilibration lengths, radial and axial temperature profiles were calculated and compared by analysing the temperature profiles.

3.1. Thermal equilibration lengths

The thermal equilibration length (TEL) is defined as the axial distance required for the blood to reach within e^{-1} of the surrounding maximum tissue temperature. Vessels with long equilibration lengths are considered thermally significant due to their ability to cause localized tissue cooling. Figure 3(*a*) displays the thermal equilibration lengths for the vessels of table 1 plotted against the product of the Peclet number (the ratio of the mean velocity and the thermal diffusivity of blood) and the vessel diameter. The product is an indicator of the convective vessel strength, and when the TEL is greater than the physical length of the vessel it results in localized tissue cooling. The TEL also depends on the thermal properties of the surrounding tissues. Figure 3(*b*) demonstrates the dependence of the TEL on perfusion for both the BHTE and ETCE models for equivalent perfusion values for a 1 mm vessel (equation (3)). An increase in tissue perfusion results in shorter thermal equilibration lengths for both models although the effect is greater for the ETCE compared with the BHTE. Both curves are characterized by a steep reduction in the TEL for lower perfusions followed by a levelling off at higher perfusions, for all vessel sizes. For a 1 mm diameter vessel

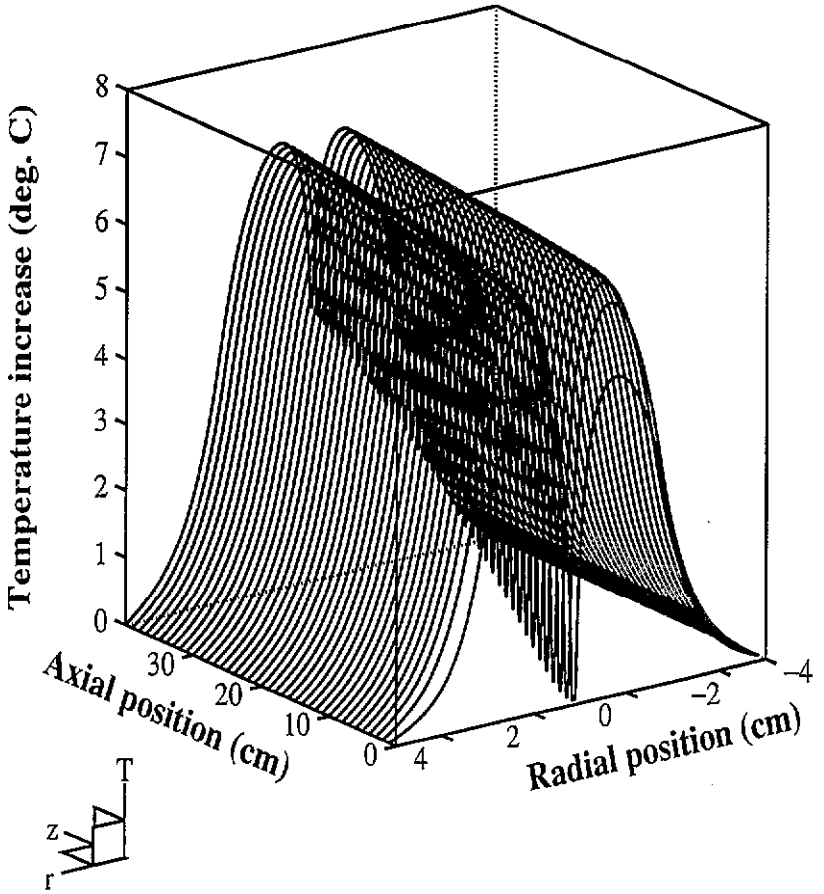

Figure 2. Steady state temperature profiles for the simulation geometry. Localized cooling of tissue is induced by the large blood vessel ($\delta = 1$ mm, $\langle u \rangle = 8$ cm s^{-1}, $w_b = 0.002$ g cm^{-3} s^{-1}, BHTE model). A parabolic blood velocity profile is assumed.

high tissue perfusion ($w_b = 0.02$ g cm^{-3} s^{-1}) can reduce the TEL by ~50% according to the BHTE and ~80% for the ETCE.

3.2. Radial temperature profiles

Tissue temperatures around large vessels are also important to model, since cooling of tumour cells close to the vessel could lead to the regrowth of the tumour (Roemer 1990). Figures 4(*a*) and (*b*) illustrate that tissue temperature increases near the vessel wall when perfusion is increased for both models. Again, the effect is greater for the ETCE model. The increase in vessel wall temperature is a direct result of the increased tissue conductivity (Crezee and Lagendijk 1992). The BHTE predicts better heating at the edges of the field for an increase in perfusion while for the ETCE the temperature profiles shift towards the vessel and edge temperatures decrease. This is due to the enhanced conduction to the vessel (and thus removal of energy). For the BHTE, higher perfusions shape the temperature field according to the power deposition pattern, giving rise to more uniform radial tissue profiles by reducing the smoothing effects of conduction. Hence, the effect of perfusion

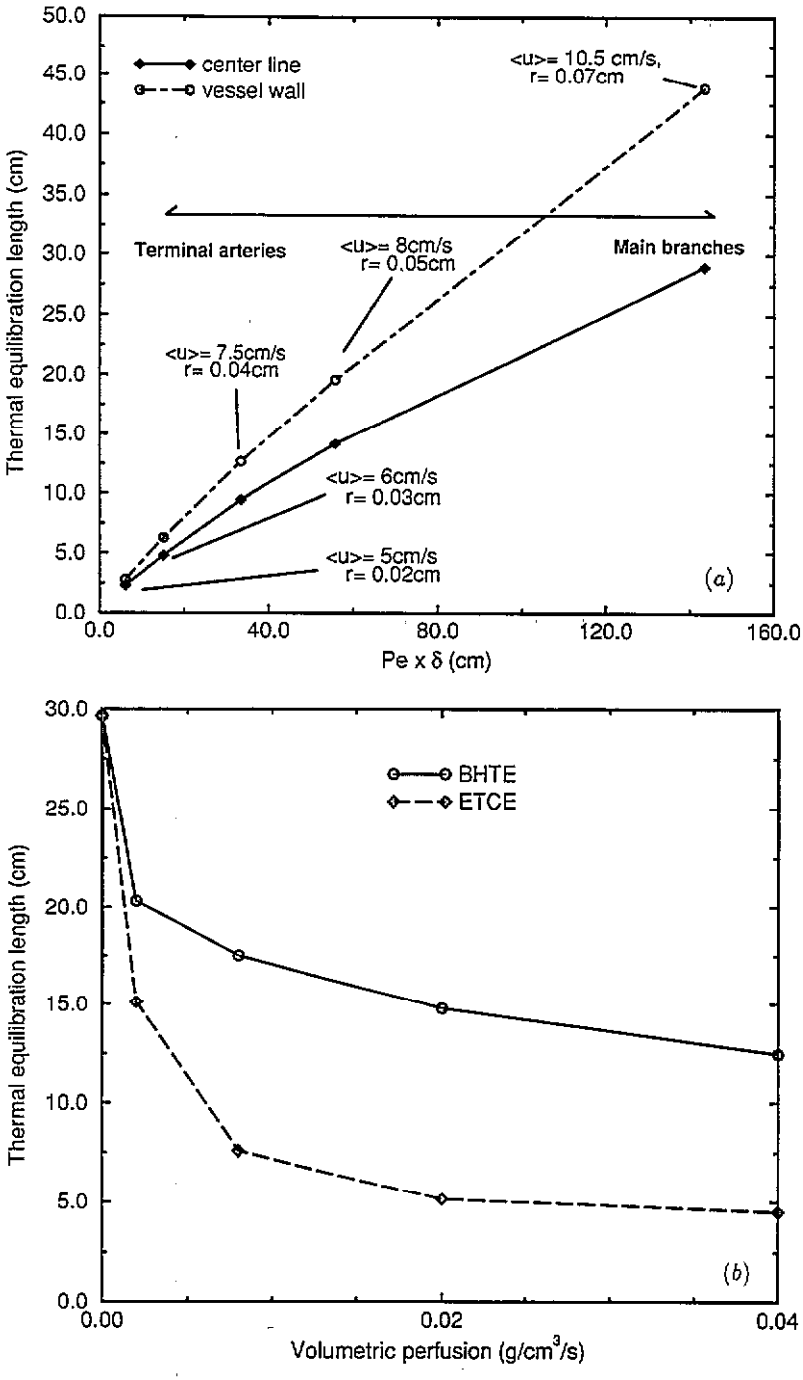

Figure 3. (*a*) TEL versus vessel size: vessels with large Peclet numbers ($Pe = \langle u \rangle / \alpha$) have long equilibration lengths resulting in localized tissue cooling. Individual vessel radii and velocities are highlighted. (*b*) Dependence of TEL on tissue perfusion, as modelled by the BHTE and ETCE models for a $\delta = 1$ mm vessel. For higher perfusions the ETCE model predicts more efficient heating for equivalent perfusion values.

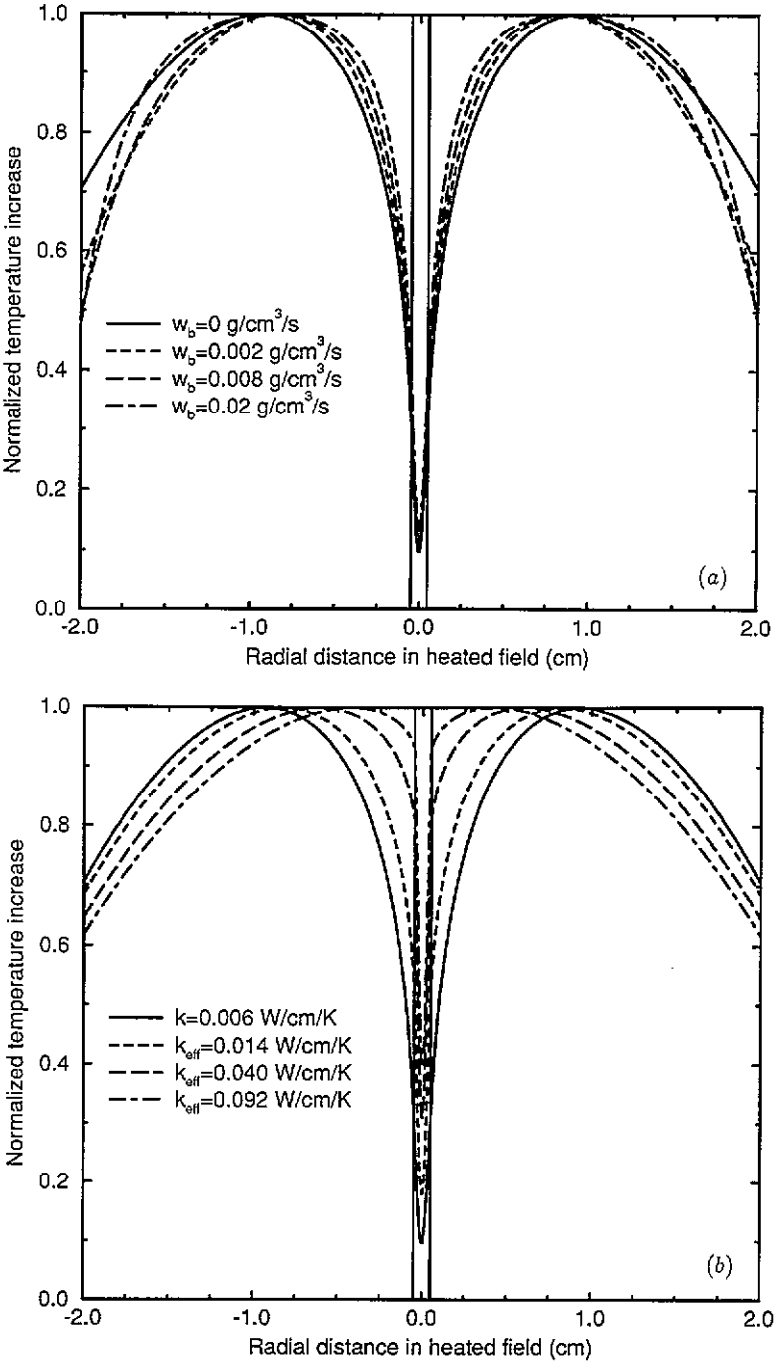

Figure 4. Simulated radial temperature profiles near vessels: effect of perfusion according to (*a*) the BHTE and (*b*) ETCE models. Profiles normalized to maximum temperature at $z = 4$ cm for a $\delta = 1$ mm vessel. Similar line styles in graphs correspond to equivalent perfusion values according to equation (3). Higher temperatures are predicted near vessels for the ETCE, especially at the vessel wall.

is to increase heat transfer to large vessels and adjacent tissue temperatures in both of the models of microvascular heat transfer. As a result, an increase in perfusion shortens the width of the radial cooling gradient reducing large vessel cooling. However, the power deposited must be increased to reach the same target temperature.

3.3. Axial temperature distributions

Figure 5 illustrates the mixing-cup temperatures (Crezee and Lagendijk 1992) of a 1 mm diameter vessel ($\langle u \rangle = 8$ cm s^{-1}). For high perfusions and according to the ETCE the axial average temperature curves are exponential and approach the limit of the Graetz Ⓣ problem† (figure 5(*b*)). Furthermore, the heat transfer coefficients approach those of the Ⓣ problem (Crezee and Lagendijk 1992). Conversely for low perfusion the axial average temperature increases linearly according to the Graetz Ⓗ problem. When microvascular heat transfer is modelled according to the BHTE, which has not been examined previously, a similar pattern occurs (figure 5(*a*)). Axial blood temperature increases exponentially and the heat transfer coefficients approach the values obtained in the Ⓣ problem. The microvasculature, according to the BHTE formulation, has the ability to modulate heat transfer to large vessels. Therefore, the effects of thermally significant vessels in poorly perfused tissues such as fat are more pronounced, regardless of which of the two models of microvasculature heat transfer is more accurate. High perfusion increases heat transfer to large vessels but simultaneously increases the power required to attain therapeutic temperatures.

3.4. Strategies to reduce large vessel cooling

3.4.1. Increasing power deposition to the vessel. A region of increased SAR was implemented as a cylinder of a radius twice the diameter of the blood vessel, simulating an idealized situation in which excess power can be deposited locally. The corresponding steady-state temperature profiles were analysed and figure 6 illustrates the results for a $\delta = 1$ mm vessel. Increasing the SAR by a factor of three or more has a substantial effect on the temperature distribution surrounding the blood vessel for the BHTE model (figure 6(*a*)). High perfusion, according to the BHTE, shapes the temperature distributions according to the SAR since the surrounding tissue acts as a strong heat sink. Therefore, increasing the SAR close to the vessel allows one to compensate for heat loss towards the vessel. For the effective conductivity model, an increase of SAR by a factor of 5 (figure 6(*b*)) produces minimal normalized temperature increases around the vessel. This is because temperature gradients created by the non-uniform SAR are rapidly smoothed by the enhanced conduction effects of perfusion. Furthermore, the T_{index} curves‡ for the effective conductivity model show minimal improvement caused by the localized increase in the SAR (data not shown).

3.4.2. Effect of heating modality The effect of heating modality was examined by assuming blood and tissue to have the same volumetric power absorption (approximating microwave heating), and by assuming no absorption by blood (modelling ultrasonic heating). Normalized temperature profiles were virtually unchanged when uniform SAR was applied

† The Graetz problem involves a fluid at temperature T_0 flowing through a cylinder that has its wall kept at a constant temperature T_w (the Graetz Ⓣ problem) or at constant heat flux (the Graetz Ⓗ problem). The solution gives the steady-state temperature and heat transfer coefficients as a function of radial and axial distance (Shah and London 1978).

‡ T_{index} is the percentage of measurements above a particular temperature plotted as a function of temperature.

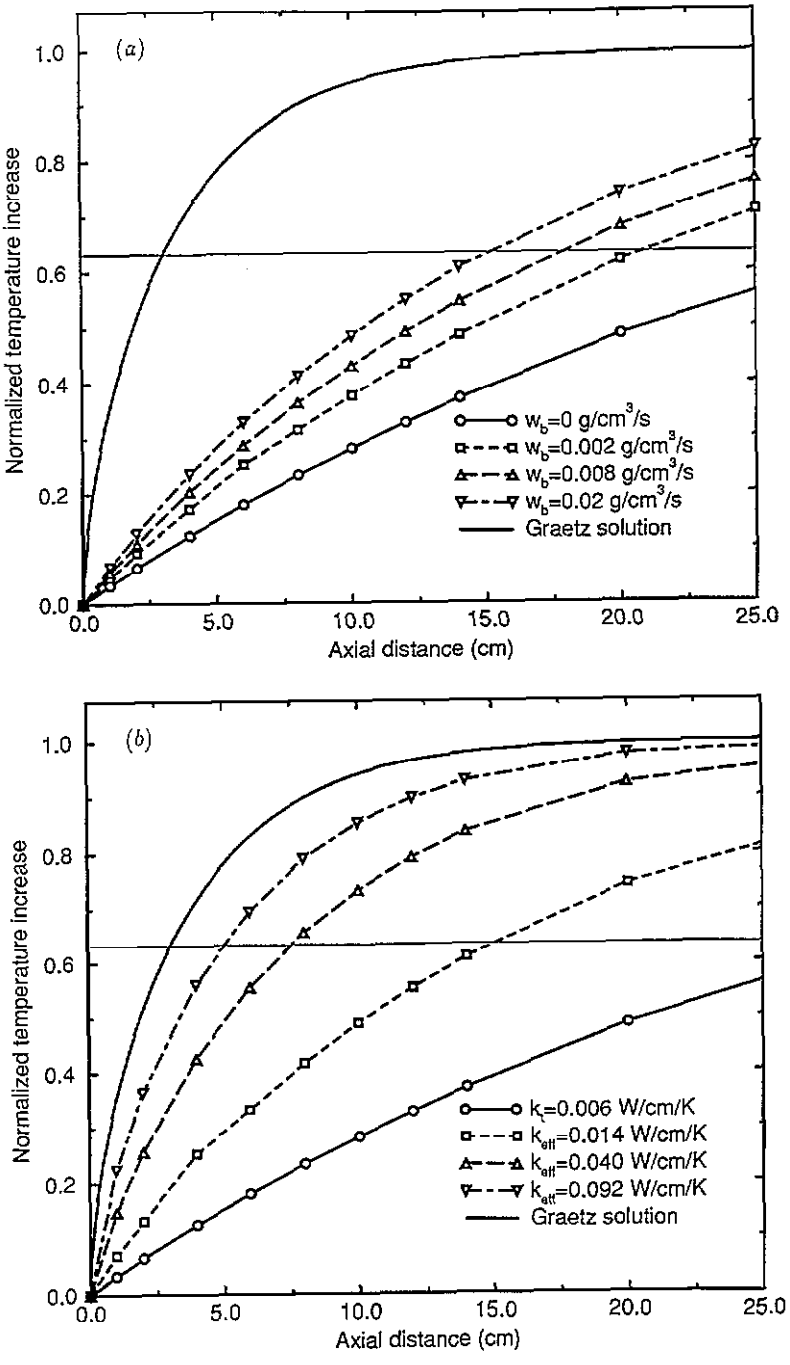

Figure 5. Normalized axial mean temperature profiles for a 1 mm vessel according to (*a*) the BHTE and (*b*) the ETCE model. Similar line styles correspond to equivalent perfusion values according to equation (3). An increase in perfusion results in shorter thermal equilibration lengths (solid horizontal lines) and better tissue heating for both models.

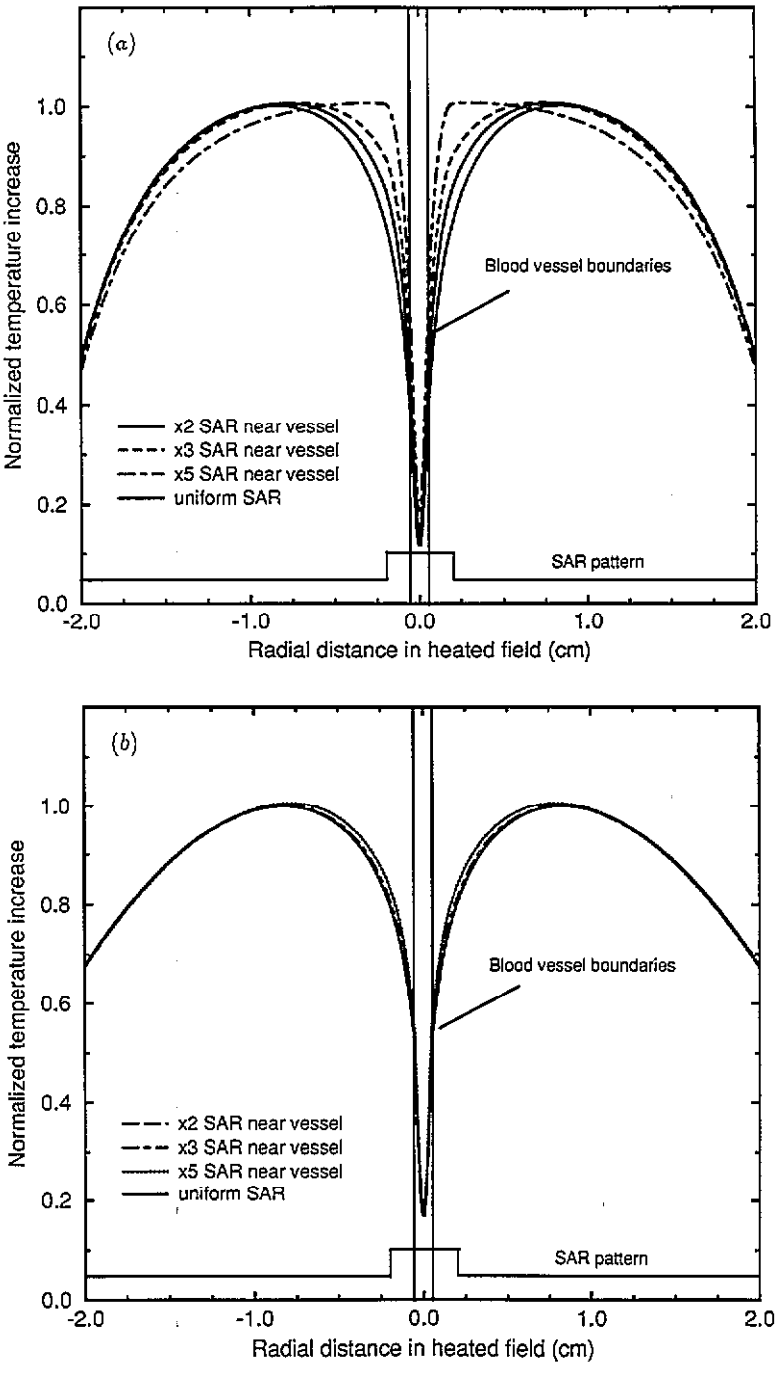

Figure 6. Radial temperature profiles near a $\delta = 1$ mm vessel: increased power deposition near the vessel for (*a*) the BHTE and (*b*) the ETCE model. Profiles are normalized to maximum temperature at $z = 4$ cm. The region of increased power deposition extends to a radius of 2δ.

to the blood, for all of the vessels sizes (data not shown). The power deposition rates could not overcome the convective strength of the thermally significant vessels and are in accordance with the finding of others (Ebadian and Zhang 1990, Roemer 1991).

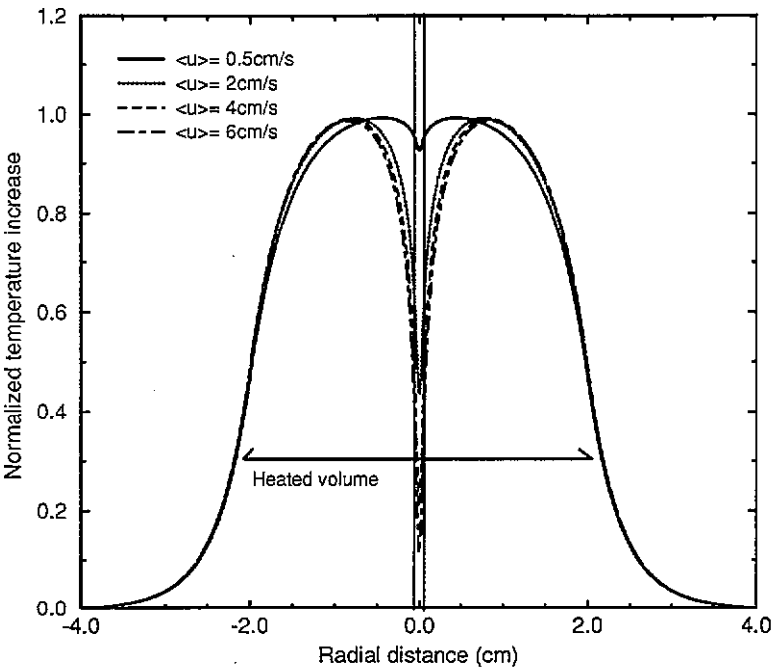

Figure 7. Temperature profiles after reduction of blood flow rates through thermally significant vessels ($\delta = 1$ mm vessel, $z = 4$ cm). When the velocity (i.e. mass flow rate) of blood through a large vessel is reduced, the surrounding tissues may reach therapeutic temperatures.

3.4.3. Vessel occlusion. Vessel occlusion was simulated by reducing the velocity of the blood through the vessel, thus representing various degrees of partial occlusion. Typical results are shown in figure 7. The radial profiles indicate that moderate occlusion (in this example for a $\delta = 1$ mm vessel and velocities of $8, 6, 4$ cm s^{-1}) does not significantly improve the temperature profiles. However, if the average velocity of the blood is drastically reduced (2.0 to 0.5 cm s^{-1}), the temperature profile is improved. For an average blood velocity of 0.5 cm s^{-1}, the vessel wall reaches to within 90% of the maximum temperature, rendering the vessel thermally insignificant. When the corresponding T_{index} curves are plotted for the simulations, a significant improvement results from the occlusion (data not shown). Greater temperature homogeneity with occlusion has been demonstrated both clinically (Levin *et al* 1994) and experimentally (Jia *et al* 1993).

4. Discussion

A novel computational model of bioheat transfer has been presented, based on the fundamental equations of energy conservation. The model is not dependent on parameters

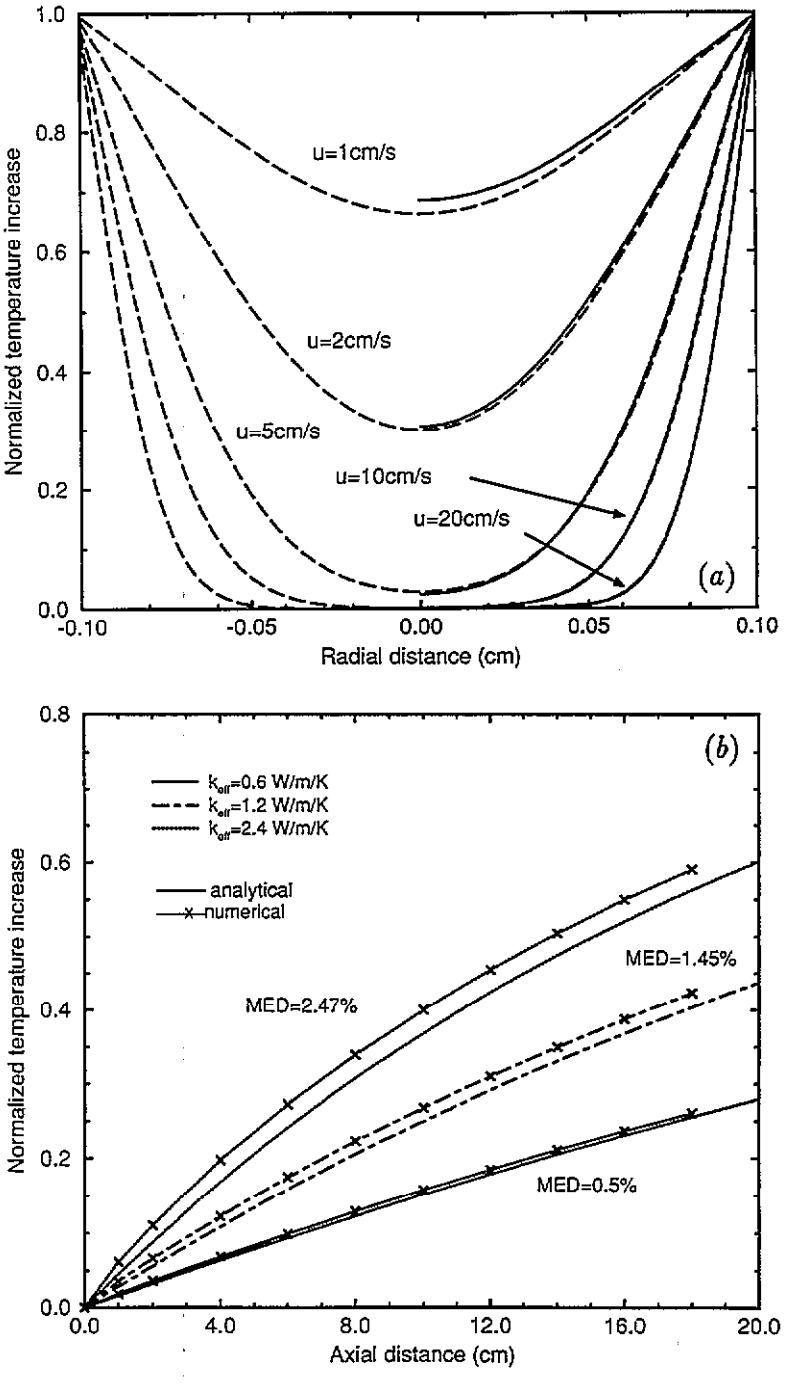

Figure 8. (*a*) Comparison of analytical and numerical solution for the Graetz problem with plug flow. The normalized temperature increase is plotted for a $\delta \sim 1$ mm vessel at a depth of $z = 4$ cm, for a range velocities. Note the small discrepancy for lower velocities (closer to the thermal entrance region). (*b*) Comparison of approximate analytical and computational solution for the conjugate problem (parabolic flow). Deviations of the solutions are attributed to the approximate nature of the analytical solution and/or numerical error. MED = maximum estimated deviation.

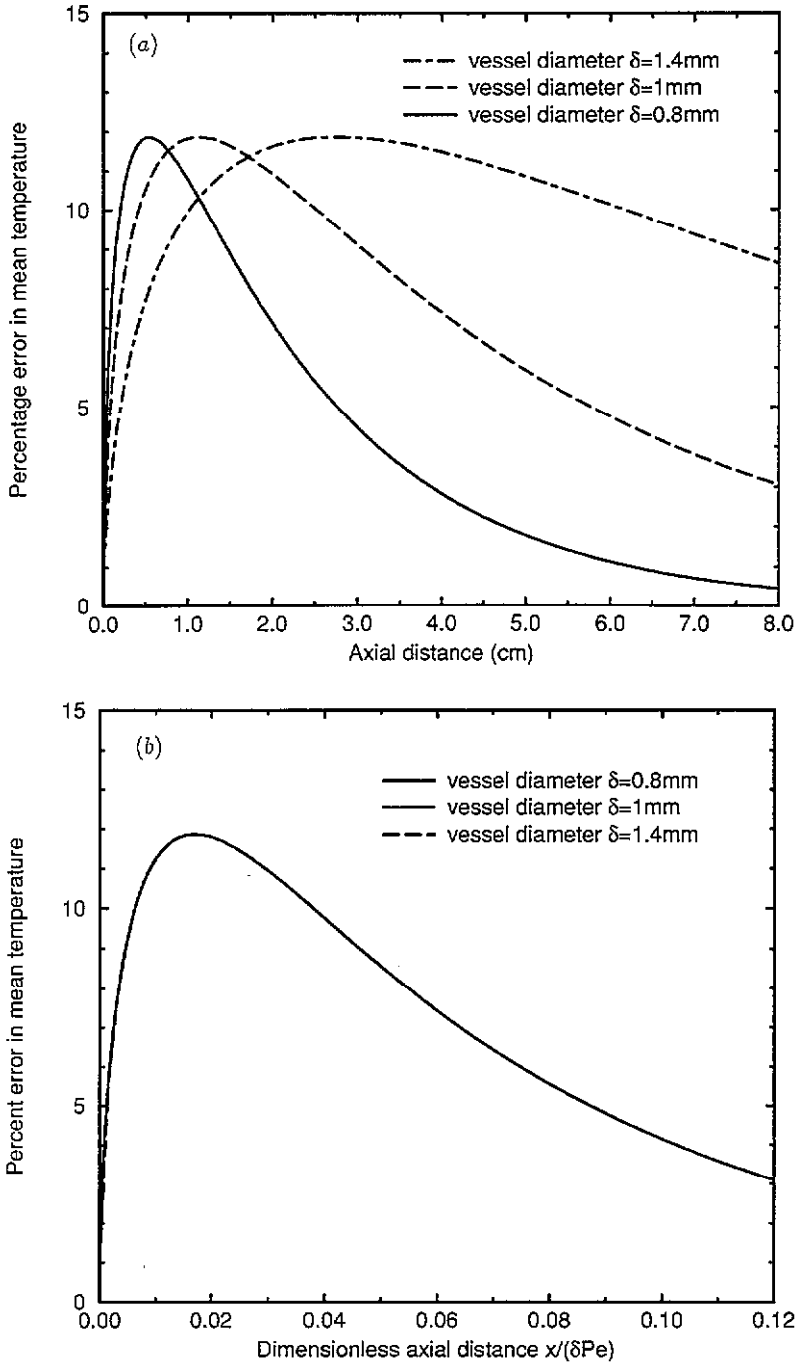

Figure 9. (*a*) Percentage error in calculated temperature when entrance effects are omitted for the Graetz constant temperature (T) problem as a function of axial distance, for three vessel sizes. (*b*) Data of previous graph when plotted against the dimensionless distance $x/(\delta\, Pe)$. In all cases the maximum error is ~12%.

such as heat transfer coefficients which have an ambiguous applicability in hyperthermia when used to model blood vessel cooling, and thus should provide more accurate predictions of temperature profiles. For example, errors due to ommission of entrance effects are estimated to be in the range of 10% (see appendix B). Perfusion of the surrounding tissue can also change the values of heat transfer coefficients. These variations, however, for the steady state and axisymmetric cylindrical geometries are bounded by the constant temperature and constant heat flux heat transfer coefficient values for the Graetz problem, for both the BHTE and ETCE models. Moreover, vessel shape can modify heat transfer to vessels; elliptical channels of eccentricity $\epsilon = 0.25$ (that may be expected in the venous system) show differences in heat transfer coefficients of almost three orders of magnitude between the endpoints of the major and minor axes, albeit the differences average out when integrated over the circumference (Basmadjian 1990). The new model however can account for all of the above factors since no assumptions are made about the heat transfer coefficients. This is predicted to be particularly important in transient calculations, since heat transfer coefficients increase when a step change in temperature occurs at the vessel wall until a steady state is reached (Basmadjian 1990). The cylindrical model in the present form, however, does not take into account the architecture of vessel networks and its effects on the temperature distributions. Therefore conclusions are based on the assumption that a large vessel acts as a dominant cooling source without interacting with other thermally significant vessels in the network. The validity of this approximation depends on the large vessel density of the target tissue (Lagendijk *et al* 1992).

Using the new model it was shown that the BHTE and ETCE differ in both predictions of temperature distributions near large vessels and optimal strategies to overcome their effects. For the ETCE, temperature peaks due to localized energy deposition are smoothed out due to conduction. In the BHTE model there is less spreading of the temperature profiles which tend to match the SAR pattern in the limits of high perfusions. Hence, when heating modalities with an adjustable or variable SAR are used to heat tissues, the ETCE model predicts smooth temperature distributions due to enhanced conduction effects, more so in the limits of large perfusions. Figure 6 illustrates these differences. Microvascular flow, in both models, increases heat flow to significant vessels. For the ETCE, an increased perfusion reduces the thermal resistance of the surrounding tissue. Similar effects are seen for the BHTE as the maximum temperature boundaries approach the vessel wall. Figures 4 and 5 illustrate the resultant increase in vessel wall and surrounding tissue temperature. Therefore, validation of microvascular heat transfer models is required before they can be used in the planning and delivery of hyperthermia, especially for well perfused organs and tumours.

Despite the inherent simplifications of the continuum models, good agreement between their predictions and experimental data have been reported in hyperthermia of dogs thighs *in vivo* (Moros *et al* 1993a), indicating that a continuum approximation for microvascular heat transfer in treatment planning may be sufficiently accurate. The authors found better agreement for the BHTE and emphasized the need to include large vessels in thermal models to interpret the temperature data obtained. Utilizing the above data, Rawnsley *et al* (1994) have shown that large vessels included in heat transfer algorithms can improve predictive ability for both the BHTE and ETCE models, albeit the BHTE had a statistically significant better ability to predict the temperature distributions. Other studies however (Crezee *et al* 1991, Crezee and Lagendijk 1990) concluded that the ETCE analysis better matched experimental data for both transient and steady-state heating. Given the difference in model predictions and the uncertainty in their applicability, it is clear that further validation studies are required.

Simulations indicate that reducing thermally significant vessel flow was the most efficient

way to ensure a uniform temperature distribution. A reduction of flow by 90% of the original flow for vessels of $\delta \sim 0.6$–1.4 mm resulted in high temperatures near the vessel (figure 7). All thermally significant vessels however cannot be occluded individually. More realistic approaches would be to either partially occlude major vessels feeding the entire region or to use vasoactive drugs to decrease blood flow to tumours. Both of these approaches have been examined clinically with varying degrees of success (Jia *et al* 1993, Prescott *et al* 1992). Tourniquets can be used to occlude blood flow to the extremities resulting in a dramatic improvement in temperature homogeneity (Levin *et al* 1994). There are however disadvantages in this approach. Selective cell killing attributed to the poor microenvironment between tumours and normal tissues would be eliminated by occlusion, requiring heating devices with excellent conformity.

The BHTE model appears to be better coupled to differences in the SAR distribution than the ETCE model therefore increasing the SAR close to the large blood vessel produced better heating patterns for the BHTE. For this approach to be clinically utilized the location and flow rates of thermally significant vessels must be known. Potential methods to image vessels and measure blood flow include Doppler ultrasound and MRI, although vessels with diameters less than 1 mm are difficult to image *in vivo*. Methods that can locally increase the SAR could be used to compensate for the cooling effects in those regions (provided the BHTE is a more accurate model). The simulations indicated that small changes in blood flow did not result in significant changes in the temperature profiles (figure 7). This allows some flexibility in thermal modelling since the input flow data need not be exact. Using a modality that deposits power in blood produced no measurable advantage for large vessels. Rapid heating of tissues has been suggested by some authors as a means to overcome the effects of perfusion and large vessels (Billard *et al* 1990, Hunt *et al* 1991). Studies with simple vessel models and geometries have demonstrated the advantages of rapid heating (Hunt *et al* 1991). Future studies with this more realistic model will include transient temperature calculations during rapid heating. Furthermore, implementation of three-dimensional codes are required for modelling situations without cylindrical symmetry.

5. Conclusions

A computational model has been developed that does not utilize heat transfer coefficients to calculate heat transfer to large vessels. Simulations using this model have shown that the surrounding perfused tissue plays a significant role in modulating heat transfer to large vessels, decreasing large vessel cooling for an increase in perfusion for both the ETCE and BHTE models. A direct comparison of the two models using experimental data to relate volumetric perfusion and effective conductivity has shown that the ETCE model predicts more effective blood heating than the BHTE for equivalent perfusion values. Furthermore, it was shown that optimal heating strategies near large vessels in perfused tissues depend on the model of microvascular heat transfer. Localized deposits of heat are smoothed by the enhanced conduction effects of the ETCE while amplified by the BHTE. As a result, even with good spatial control of the SAR, the temperature distributions near large vessels may be suboptimal if tissue microvascular heat transfer behaves as an effective conductivity, especially for poorly perfused tissues. Reducing the volumetric flow through thermally significant vessels appears to be the most promising strategy to reduce localized cooling of large vessels.

Acknowledgments

We wish to thank the National Cancer Institute of Canada, Medical Research Council and Ontario Cancer Treatment and Research Foundation for financial support of this work. The authors also wish to thank C C Christara of the Department of Computer Science of the University of Toronto for useful discussions.

Appendix A

Analytical solutions to the conjugate problem as posed by equations (1) and (2) are not available. Therefore, solutions of simplified problems must be sought. The Graetz problem was used as a benchmark to compare analytical and computational solutions in the blood domain (i.e the analytical solution of equation (1) for a constant vessel wall temperature). The computational geometry was set to the problem specifications (e.g. no power deposition, constant wall temperature). Analytical expressions were taken from Shah and London (1978). Figure 8*(a)* indicates good agreement between the radial profiles of the computational and analytical solution. Inaccuracy is expected to be greatest in the entrance region for the vessels, and thus for lower velocities (at a given depth) the error is greater. Comparison of the tissue domain with analytical solutions without fluid flow also produced excellent agreement (Kolios 1994). To evaluate the conjugate problem in which the fluid and tissue domains are coupled, an analytical solution derived by Crezee and Lagendijk (1992) was used as a benchmark, using $Nu = 3.66$ and a ratio of the radius at maximum temperature versus radius of vessel (b/a) of 20. Figure 8(b) demonstrates a discrepancy between the two solutions that may be attributed to the fact that the analytical solution does not account for entrance effects or to computational errors due to the conductivity mismatch at the tissue vessel boundary. The trends, however, of the two curves are similar and their maximum deviation does not exceed 6% for a range the range of effective conductivities examined.

Appendix B

Entrance effects enhance heat transfer to fluids that are not fully thermally developed. An approximate error estimate for the average fluid temperature when entrance effects are omitted can be calculated for the Ⓣ case. If entrance effects are excluded there is no axial dependence of the radial fluid temperature profiles and the energy equation for the Graetz problem becomes (equation (1))

$$\dot{m} c_b \frac{dT_b}{dz} = 2q\pi r_0 \tag{B1}$$

where q is the heat flow to the vessel. The above equation has a solution for $T_b(z = 0) = 0$, wall temperature T_w and $Nu =$ constant

$$T_b(z) = T_w \left\{1 - \exp\left[-2(Nu\, Pe\, z/r_0)\right]\right\} \tag{B2}$$

where Pe is the Peclet number. Equation (B2) can be subtracted from the Graetz solution to calculate the error from the omission of entrance effects (assuming a Nu number of 3.66). Figures 9(a) and (b) display the difference between the Graetz solution and the solution of (B2) plotted against the axial and dimensionless axial distance, respectively. Excluding entrance effects underestimates the average blood temperature by a maximum of 12%, and persists for significant distances along large vessels. The rate of heat transfer is greater in

the entrance region since the radial temperature profiles are not fully developed. At larger axial distances, the accumulative contribution from the entrance region is small compared to the contribution from the rest of the vessel and thus the solutions converge.

References

Ames W F 1977 *Numerical Methods for Partial Differential Equations* (New York: Academic)

Baish J W 1992 Formulation of a statistical model of heat transfer in perfused tissue *Advances in Biological Heat and Mass Transfer 1992* vol HTD-231, ed J J McGrath (New York: ASME) pp 135–40

Basmadjian D 1990 The effect of flow and mass transport in thrombogenesis *Ann. Biomed. Eng.* **18** 685–709

Billard B E, Hynynen K and Roemer R B 1990 Effects of physical parameters on high temperature ultrasound hyperthermia *Ultrasound Med. Biol.* **16** 409–20

Bowman H F, Curley M G, Newman W H, Summit S C, Chang S, Hansen J, Herman T S and Svensson G K 1989 Use of effective conductivity for hyperthermia treatment planning *Bioheat Transfer–Applications in Hyperthermia, Emerging Horizons in Instrumentation and Modeling* vol HTD 126/BED 12, ed J J McGrath (New York: ASME) pp 23–8

Chato J C 1980 Heat transfer to blood vessels *J. Biomech. Eng.* **102** 110–8

Chen Z P and Roemer R B 1992 The effects of large blood vessels on temperature distributions during hyperthermia *J. Biomech. Eng.* **114** 473–81

Crezee J and Lagendijk J J W 1990 Experimental verification of bio-heat transfer theories: measurement of temperature profiles around large artificial vessels in perfused tissue *Phys. Med. Biol.* **35** 905–23

——1992 Temperature uniformity during hyperthermia: the impact of large vessels *Phys. Med. Biol.* **37** 1321–37

Crezee J, Mooibroek J, Bos C K and Lagendijk J J W 1991 Interstitial heating: experiments in artificially perfused bovine tongues *Phys. Med. Biol.* **36** 823–33

Duck F A 1990 *Physical Properties of Tissues: A Comprehensive Reference Book* (San Diego, CA: Academic)

Dutton A W 1993 A finite element solution to conjugated heat transfer is tissue using magnetic resonance angiography to measure the *in vitro* velocity field *PhD Thesis* University of Arizona

Ebadian M A and Zhang H Y 1990 Effects of heat generation and axial heat conduction in laminar flow inside a circular pipe with a step change in wall temperature *Int. Commun. Heat Mass Transfer* **17** 621–35

Hunt J W, Lalonde R J, Ginsberg H, Urchuck S and Worthington A 1991 Rapid heating: critical theoretical assessments of thermal gradients found in hyperthermia treatments *Int. J. Hyperthermia* **7** 703–18

Jia Z Q, Worthington A E and Hunt J W 1993 The effects of artery occlusion on the temperature distribution under hyperthermia in the animals kidneys *in vivo Paper abstracts of the 41st Annual Meeting of the Radiation Research Society (Dallas, TX, 1993)* p 12

Kolios M C 1994 Models of bioheat transfer during hyperthermia *Masters Thesis* University of Toronto

Kolios M C, Sherar M D, Worthington A E and Hunt J W 1994 Modeling temperature gradients near large vessels in perfused tissues *Fundamentals of Biomedical Heat Transfer* vol HTD-295, ed M A Ebadian and P H Oosthuizen (New York: ASME) pp 23–30

Lagendijk J J W, Crezee J and Mooibroek J 1992 Progress in thermal modelling development *Proc. 6th Int. Cong. on Hyperthermic Oncology; Hyperthermic Oncology (Tucson, AZ, 1992)* vol 2, ed E W Gerner and T C Cetas, pp 257–61

Lemons D E, Chien S, Crawshaw L I, Weinbaum S and Jiji L M 1987 Significance of vessel size and type in vascular heat transfer *Am. J. Physiol.* **253** R128–35

Levin W, Sherar M D, Cooper B, Hill R P, Hunt J W and Liu F F 1994 The effect of vascular occlusion on tumor temperatures during superficial hyperthermia *Int. J. Hyperthermia* **10** 495–505

Mooibroek J and Lagendijk J J W 1991 A fast and simple algorithm for the calculation of convective heat transfer by large vessels in three-dimensional inhomogeneous tissues. *IEEE Trans. Biomed. Eng.* **BE-38** 490–501

Moros E G, Dutton A W, Roemer R B, Burton M and Hynynen K 1993a Experimental evaluation of two simple thermal models using hyperthermia *in vivo Int. J. Hyperthermia* **9** 581–98

Moros E G, Straube W L and Myerson R J 1993b Finite difference vascular model for 3-d cancer therapy with hyperthermia *Advances in Biological and Heat and Mass Transfer* vol HTD-268, ed R B Roemer (New York: ASME) pp 107–11

Patankar S V 1980 *Numerical Heat Transfer and Fluid Flow* (Washington, DC: Hemisphere)

Prescott D M, Samulski T V, Dewhrist M W, Page R L, Thrall D E, Dodge R K and Oleson J R 1992 Use of nitroprusside to increase tissue temperature during local hyperthermia in normal and tumor-bearing dogs *Int. J. Radiat. Oncol. Biol. Phys.* **23** 377–85

Rawnsley R J, Roemer R B and Dutton A W 1994 The simulation of discrete vessel effects in experimental hyperthermia *J. Biomech. Eng.* **116** 256–62

Roemer R B 1990 The local tissue cooling coefficient: a unified approach to thermal washout and steady-state 'perfusion' calculations *Int. J. Hyperthermia* **6** 421–30

——1991 Optimal power deposition in hyperthermia I. The treatment goal: the ideal temperature distribution II. The role of large blood vessels *Int. J. Hyperthermia* **7** 317–41

Shah R K and London A L 1978 *Laminar Flow Forced Convection in Ducts* (New York: Academic)